

## Adsorption Of $\text{NO}_3^-$ -N And $\text{PO}_4^{3-}$ -P in Aqueous Solution Using Granular Activated Charcoal (Gac)

Yong Pyo Hong and Keon Sang Ryo<sup>\*</sup>

Department of Applied Chemistry, Andong National University, Andong 760-749, Korea.

ksr@andong.ac.kr

### ABSTRACT

In this study, adsorption of  $\text{NO}_3^-$ -N and  $\text{PO}_4^{3-}$ -P on granular activated charcoal (GAC) was investigated depending on pH, agitation time, GAC dosage, adsorption capacity and adsorption isotherms by employing batch adsorption type. The GAC was characterized by thermogravimetric analysis (TG-DTA), scanning electron micrograph coupled with energy-dispersive X-ray spectroscopy (SEM-EDX) and BET surface area analyzer. The GAC exhibited nearly similar adsorption equilibrium time. Both  $\text{NO}_3^-$ -N and  $\text{PO}_4^{3-}$ -P appeared to approach equilibrium after approximately 4 h of agitation time. In the adsorption equilibrium, the removal efficiencies of  $\text{NO}_3^-$ -N and  $\text{PO}_4^{3-}$ -P were found to be 14.6-66.0 % and 52.4-99.0 %, respectively. The adsorption data for  $\text{NO}_3^-$ -N and  $\text{PO}_4^{3-}$ -P was correlated to Freundlich and Langmuir isotherm model and the equilibrium data was fitted well to the Langmuir isotherm model due to their higher correlation coefficient ( $R^2$ ) value. The Langmuir adsorption capacity was 1.54 and 2.56  $\text{mg g}^{-1}$  for  $\text{NO}_3^-$ -N and  $\text{PO}_4^{3-}$ -P, respectively, which suggests that the GAC is a good adsorbent for removal of  $\text{NO}_3^-$ -N and  $\text{PO}_4^{3-}$ -P from water.

**Keywords:** Granular activated charcoal,  $\text{NO}_3^-$ -N,  $\text{PO}_4^{3-}$ -P, Adsorption, Isotherm

### 1. INTRODUCTION

Nitrogen and phosphorous have been usually considered to be limiting nutrients in relation to eutrophication of water bodies including reservoirs, lakes, streams, rivers, estuaries and coastal waters [1,2]. The agricultural and industrial activities of human have continually impoured them into water. As a result, they have exceeded the specified acceptable limits in many countries of the world. Their enrichment in water brings about occasionally the algal blooms. The high growths of algae in aquatic system can cause a harmful effect on water quality and also obstruct the water treatment processes. The Korean Ministry of the Environment has set a strict control of less than 0.6  $\text{mg L}^{-1}$  of nitrogen and 0.025  $\text{mg L}^{-1}$  of phosphorous in the water to escape from eutrophication problems. Generally, the principal nitrogen and phosphorous in water mainly exist in nitrate and phosphate. A lot of studies have been introduced to the removal of nitrate and phosphate in wastewater using biological and chemical treatments over decades [3-6]. However, biological treatments have shown unstable and insufficient efficiencies in removing nitrate and phosphate from wastewater. Besides, they have considerable difficulty in controlling microorganism due to the long-term biodegradation. Chemical treatments have also been widely used as a viable alternative to biological treatments. Nevertheless, their applicability of wastewater treatment has been limited due to the high cost of chemical additives and the production of chemical sludge.

Adsorption can become a quite popular method owing to the simplicity, the absence of sludge and the availability of a wide range of adsorbents. The important key to success and failure of adsorption depends mainly on the choice of a proper adsorbent. Generally, adsorbent must satisfy the following preconditions [7,8]: (1) an easily available material; (2) a low-cost; (3) no hazardous pollutants; (4) an easy recycle; (5) a high physical strength. Many investigators have attempted the removal of nitrate and phosphate from wastewater using various adsorbents such as activated alumina, ion exchange resin, synthetic zeolite, goethite, fly ash, red mud and loess [9-14]. Activated charcoal, or activated carbon, is an amorphous form of carbon prepared from incomplete combustion of carbonaceous organic matter such as peat, coal, wood, coconut shell, or petroleum. It is activated by an oxidizing gas flow at high temperature passed over its surface to make a fine network of pores, producing a material with large surface area and high affinity for various substances [15]. Activated charcoal has been widely used in wastewater treatment for a long time and proven to be one of the most effective and reliable adsorbents [16-18]. Although the high production cost of activated charcoal makes its use

restricted, it may be still a favorite choice as an adsorbent for removal of nitrate and phosphate from wastewater because of its high surface area and pore volume and size, along with convenient regeneration of spent carbon.

The present study is to explore the possibility of utilizing activated charcoal for removal of nitrate and phosphate from aqueous solution. Adsorption process of activated charcoal was carried out with a batch-type. The effect of various operating conditions such as pH, initial concentrations, adsorbent dose and agitation time was systematically investigated. To figure out the adsorption behavior, the experimental data was fitted to the Freundlich and Langmuir isotherm models. Furthermore, analysis instruments such as a thermogravimetric analysis (TGA), a scanning electron micrograph coupled with energy-dispersive X-ray spectroscopy (SEM/EDX) and a BET surface area analyzer were used to characterize activated charcoal.

## **2. MATERIALS AND METHODS**

### **2.1. Materials and chemicals**

Granular activated charcoal (GAC) provided by Yakuri Pure Chemicals Co., Ltd., Kyoto, Japan was used as an adsorbent in this adsorption study. The size of GAC is between 8 and 32 mesh. The monobasic potassium phosphate ( $\text{KH}_2\text{PO}_4$ ) and potassium nitrate ( $\text{KNO}_3$ ) as a source of  $\text{NO}_3^-$ -N and  $\text{PO}_4^{3-}$ -P were purchased from Duksan Pharmaceutical Co., Ltd, Gyeonggi-do, Korea and Daejung Chemicals & Metals Co., Ltd, Gyeonggi-do, Korea, respectively. They are all reagent grade above 99.0% of purity. The stock solutions of phosphate and nitrate containing 1000 mg P/L and 1000 mg N/L were prepared by dissolving in distilled water. Phosphate and nitrate working solutions of different concentrations were produced by diluting stock solutions with distilled water and 0.01 M KCl was added for adjusting their ionic strength.

### **2.2. Adsorption studies of GAC**

The effect of agitation time, pH, initial concentrations and GAC dosage on the removal of phosphate and nitrate from aqueous solution was investigated in a series of batch-sorption experiments. For these studies, each 250 mL flask was filled with 100 mL of phosphate and nitrate solutions and placed in a thermostatic shaker. A certain amount of GAC was added into flasks and then agitated at 200 rpm from 10 min until 24 h. The initial concentrations of phosphate and nitrate were in the range of 0.5 to 5.0 mg  $\text{L}^{-1}$  and 1.0 to 10.0 mg  $\text{L}^{-1}$ , respectively. At specific time intervals, a fraction of the aqueous solution was withdrawn from the flask and centrifuged with a centrifugal separator at 3500 rpm for 30 min. Subsequently, the supernatant was filtered through a 0.47  $\mu\text{m}$  filter (GF/C<sup>TM</sup>, Whatman) to remove the GAC particles before analytical measurements were made. The concentrations of nitrate and phosphate in filtrate were determined by a UV/Visible spectrophotometer (Carry 5000, Varian Technologies, Australia) at the corresponding  $\lambda_{\text{max}} = 880 \text{ nm}$  and 215 nm, respectively. The pH of aqueous solution before and after experiment was measured using a pH meter.

### **2.3. Analytical measurements**

The mass change on GAC according to temperature was examined using a thermogravimetric analysis (TG-1280, Rigaku, Japan), from 30 °C to 900 °C with 20 °C/min heating rate under  $\text{N}_2$  environment. The surface texture of GAC was performed with a scanning electron micrograph (SEM, Vega II LMU, Tescan, Czech) coupled with energy-dispersive X-ray spectroscopy (EDX, X-MaxN, Oxford, UK). Specific surface area and pore volume of the GAC were determined by  $\text{N}_2$  adsorption isotherm at 77 K with a specific surface area analyzer (3 Flex, Micrometrics, Germany). Prior to  $\text{N}_2$  adsorption, GAC was degassed under vacuum at 200 °C for 12 h. The total surface area and micropore volume at  $P/P_0 = 0.3$  were determined by applying the Brunauer–Emmett–Teller (BET) and t-plot equation, respectively. The value of mesopore volume was obtained by deducting the micropore volume out of the total pore volume. According to the pore size distribution of IUPAC, pore sizes between 2–50 nm and < 2 nm are classified as mesopore and micropore, respectively. The pH value of GAC were measured by using a pH meter (Radiometer PHM 250 ion analyser, USA) combined with a glass electrode in the 1:2.5 suspension of GAC and distilled water after stirring for 10 min.

### 3. RESULTS AND DISCUSSION

#### 3.1. Characterization of GAC

The TGA result (Fig. 1) exhibited one major decomposition of 93.45 % in the range of 450-720 °C. The decomposition can be attributed to the evolution of CO<sub>2</sub>. It is seen that the stoichiometrical weight of GAC consists of H<sub>2</sub>O of 3.62 %, volatile organics and H<sub>2</sub> of 1.47%, C of 93.45 % and inorganics of 1.46 %. Fig. 2 represents SEM image of particles of GAC magnified to 5000 times. As seen, GAC showed a smoothly looking appearance that is revealed the presence of highly scattered irregular pores on the surface of the GAC particles. The EDX spectrum of GAC shows the existence of C and O as major elements along with Na, S and Cl. Table 1 shows the elemental content of GAC as determined by EDX. It was found that the GAC is comprised of significant C content compared to other elements. The general properties of GAC are shown in Table 2. The BET surface area of GAC was found to be 1228.87 m<sup>2</sup>g<sup>-1</sup> and its micropore pore volume was 0.49 cm<sup>3</sup>g<sup>-1</sup>. The measured pH value of GAC was 5.8, indicating an weak acidic nature.

#### 3.2. Effect of contact time and initial concentration

The batch adsorption studies were carried out with different initial NO<sub>3</sub><sup>-</sup>-N and PO<sub>4</sub><sup>3-</sup>-P concentrations in the range of 1.0-10.0 and 0.5-5.0 mg L<sup>-1</sup>, respectively while maintaining 1.0 g of GAC during 10 min - 24 h. Fig. 4 and 5 represent the removal efficiencies (%) of GAC for initial NO<sub>3</sub><sup>-</sup>-N and PO<sub>4</sub><sup>3-</sup>-P concentrations plotted as a function of agitation time. As shown in Fig. 4 and 5, the GAC exhibited nearly similar adsorption equilibrium time for both NO<sub>3</sub><sup>-</sup>-N and PO<sub>4</sub><sup>3-</sup>-P. The agitation time corresponding to the maximum adsorption is usually considered as the adsorption equilibrium time. The adsorption equilibrium for NO<sub>3</sub><sup>-</sup>-N and PO<sub>4</sub><sup>3-</sup>-P occurred within around 4 h. After the equilibrium, the remaining concentration of NO<sub>3</sub><sup>-</sup>-N and PO<sub>4</sub><sup>3-</sup>-P in aqueous solution was nearly unchanged. The removal efficiencies of NO<sub>3</sub><sup>-</sup>-N and PO<sub>4</sub><sup>3-</sup>-P on GAC were calculated by using the following equation:

$$\text{Removal efficiency (\%)} = \frac{100K_d}{\left(K_d + \frac{V}{m}\right)} \quad (1)$$

$$K_d = \frac{\text{Amount of sorbate adsorbed on adsorbent}}{\text{Amount of sorbate remaining in solution}} \times \frac{V}{m} \quad (2)$$

Where  $V$  (mL) is the volume of the solution and  $m$  (g) is the mass of the adsorbent.

The adsorption amount of NO<sub>3</sub><sup>-</sup>-N and PO<sub>4</sub><sup>3-</sup>-P on GAC was highly concentration dependent. The removal efficiencies displayed a tendency to be lower with increasing initial concentration of NO<sub>3</sub><sup>-</sup>-N and PO<sub>4</sub><sup>3-</sup>-P. Based on the initial concentrations, roughly 14.6-66.0 % and 52.4-99.0 % of removal efficiencies for NO<sub>3</sub><sup>-</sup>-N and PO<sub>4</sub><sup>3-</sup>-P at equilibrium was accomplished by GAC, respectively.

#### 3.3. Adsorption isotherm

The commonly used Freundlich and Langmuir adsorption isotherm models in this study were employed to find out the adsorption mechanism. Adsorption isotherms express the distribution of adsorbates between adsorbent and the liquid phase when adsorption equilibrium is reached at a constant temperature and provide parameters for designing and optimizing the adsorption system.

The Freundlich isotherm, which is an empirical equation for multi-layer adsorption of adsorbate onto heterogeneous surfaces of adsorbent [19], is expressed as follows:

$$q_e = k_f(c_e)^{1/n} \quad (3)$$

Where,  $q_e$  ( $\text{mg g}^{-1}$ ) is the amount of adsorbate adsorbed by adsorbent at equilibrium and  $c_e$  ( $\text{mg L}^{-1}$ ) is the equilibrium concentration of adsorbate in solution. The  $k_f$  is the Freundlich constant related to adsorption capacity. The  $1/n$  is a measure of the adsorbent affinity for the adsorbate or surface heterogeneity, becoming more heterogeneous as its value gets closer to 0. For linearization of the data, the Freundlich equation is written in logarithmic form:

$$\log q_e = \log k_f + \frac{1}{n} \log c_e \quad (4)$$

A linear plot of  $\log q_e$  versus  $\log c_e$  yields a slope  $1/n$  and an intercept of  $\log k_f$ .

The Langmuir isotherm assumes mono-layer adsorption on homogeneous surface of adsorbent with no interaction between adjacent adsorbed adsorbates [20]. It implies that, there is a finite number of adsorption sites present on the adsorbent, and after filling up the present sites, no adsorption occurs further. The Langmuir isotherm is written as:

$$\frac{c_e}{q_e} = \frac{1}{Qb} + \frac{c_e}{Q} \quad (5)$$

Where,  $Q$  ( $\text{mg g}^{-1}$ ) and  $b$  ( $\text{L mg}^{-1}$ ) are empirical constants representing the mono-layer adsorption capacity and the energy of adsorption, respectively, and the plot of  $c_e/q_e$  against  $c_e$  yields a straight line with the slope  $1/Q$  and the intercept  $1/Qb$ .

The plots of Freundlich and Langmuir isotherm for  $\text{NO}_3^-$ -N and  $\text{PO}_4^{3-}$ -P on GAC at 298 K were presented in Fig. 6-9, and the corresponding isotherm parameters are listed in Table 3. It was observed that the experimental data for  $\text{NO}_3^-$ -N and  $\text{PO}_4^{3-}$ -P adsorption deviates more in case of the Freundlich than Langmuir plot. This is further verified by the correlation coefficient ( $R^2$ ) value, shown in Table 3, of the linear plots. It is evident that the Langmuir isotherm fits the experimental data better than the Freundlich isotherm, suggesting the good applicability of the Langmuir model to this adsorption.

The Langmuir adsorption capacity of GAC for adsorption of  $\text{NO}_3^-$ -N and  $\text{PO}_4^{3-}$ -P was found to be 1.54 and 2.56  $\text{mg g}^{-1}$ , respectively. In case of Langmuir isotherm model, the type of adsorption is classified by a dimensionless constant separation factor  $r$  [21] which is given by the following equation:

$$r = \frac{1}{1 + bc_i} \quad (6)$$

Where,  $c_i$  ( $\text{mg L}^{-1}$ ) is the initial adsorbate concentration. The  $r$  values greater than 1 indicate unfavorable type of adsorption while the values between 0 and 1 represent favorable adsorption. In this study, the  $r$  values lie within 0.08-0.48 and 0.01-0.093 for initial  $\text{NO}_3^-$ -N and  $\text{PO}_4^{3-}$ -P concentrations, respectively. These values reflect that GAC favors the adsorption of  $\text{NO}_3^-$ -N and  $\text{PO}_4^{3-}$ -P from aqueous solution in the studied concentration ranges.

#### 4. CONCLUSIONS

The capability of GAC for adsorption of  $\text{NO}_3^-$ -N and  $\text{PO}_4^{3-}$ -P from aqueous solution was evaluated. The observed adsorption data showed that GAC has a similar adsorption equilibrium time (4 h) for both  $\text{NO}_3^-$ -N and  $\text{PO}_4^{3-}$ -P. The adsorption amount of  $\text{NO}_3^-$ -N and  $\text{PO}_4^{3-}$ -P by GAC was dependant on the initial concentration. It was observed that the removal efficiency decreased with increasing the initial concentration of  $\text{NO}_3^-$ -N and  $\text{PO}_4^{3-}$ -P. At investigated initial concentration ranges, approximately 14.6-66.0 % and 52.4-99.0 % of removal efficiencies for  $\text{NO}_3^-$ -N and  $\text{PO}_4^{3-}$ -P at equilibrium was achieved by GAC, respectively. The adsorption isotherm study showed that the adsorption of  $\text{NO}_3^-$ -N and  $\text{PO}_4^{3-}$ -P on GAC follows the Langmuir isotherm model due to their higher correlation coefficient ( $R^2$ ) value than the Freundlich isotherm model. The Langmuir adsorption capacity of GAC for the uptake of  $\text{NO}_3^-$ -N and  $\text{PO}_4^{3-}$ -P was found to be 1.54 and 2.56  $\text{mg g}^{-1}$ , respectively.

## **ACKNOWLEDGMENTS**

This work was supported by a Research Grant of Andong National University.

## **REFERENCES**

1. Xiong, J., Qin, Y., Islam, E., Yue, M., wang, W., 2011. *Desalination* 276, 317-321.
2. Lee, S. H., Kim, C. K., park, J. G., Choi, D. K., Ahn, J. H., 2017. *J. Korean Soc. Environ. Eng.* 39(5), 303-309.
3. Choi, J., Lee, S., Park, K., Lee, K., Kim, K., Kim, D., Lee, S., 2011. *Desalination* 266, 281-285.
4. Johir, M.A.H., George, J., Vigneswaran, S., Kandasamy, J., Grasmick, A., 2011. *Desalination* 275. 197-202.
5. Ding, A., Qu, F., Liang, H., Ma, Jun., Han, Z., Yu, H., Guo, S., Li, G., 2013. *Chem. Eng. J.* 223, 908-914.
6. Littler, J., Geroni, J.N., Sapsford, D.J., Coulton, R., Griffiths, A.J., 2013. *Chemosphere* 90, 1533-1538.
7. Urano, K., Tachikawa, H., 1991. *Ind. Eng. Chem. Res.* 30, 1893-1896.
8. Onyango, M.S., Kuchar, D., Kubota, M., Matsuda, H., 2007. *Ind. Eng. Che. Res.* 46, 894-90.
9. Brattebo, H., Odegaard, H., 1986. *Water Res.* 20, 977-986.
10. Chen, J.P., Chau, M.L., Zhang, B., 2002. *Waste Manage.* 22, 711-719.
11. Ler, A., Stanforth, R., 2003. *Environ. Sci. Technol.* 37, 2694-2700.
12. Ugurlu, A., Salman, B., 1998. *Environ. Int.* 24, 911-918.
13. Huang, W., Wang, S., Zhu, Z., Li, L., Yao, V., Rudolph, V., Haghseresht, F., 2008. *J. Hazard. Meter.* 158, 4-42.
14. Park, J.H., Jung, D.I., 2011. *Desalination* 269, 104-110.
15. Ucer, A., Uyanik, A., Aygun, S. F., 2006. *Separation and purification Technology* 47, 113-118.
16. Gomez, V., Larrechi, M.S., Callao, M.P., 2007. *Chemosphere* 69, 1151-1158.
17. Richard D., de Lourdes Delgado Nunez, M., Schweich, D., 2009. *Chem. Eng. J.* 148, 1-7.
18. Richard D., de Lourdes Delgado Nunez, M., Schweich, D., 2010. *Chem. Eng. J.* 158, 213-219.
19. Mohanthy, K., Naidu, J.T., Meikap, B.C., Biawas, M.N., 2006. *Ind. Eng. Chem. Res.* 45, 5165-5171.
20. Nadaroglu, H., Kalkan, E., Demir, N., 2010. *Desalination* 251, 90-95.
21. Palanisamy, P.N., Sivakumar, P., 2009. *Desalination* 249, 388-397.

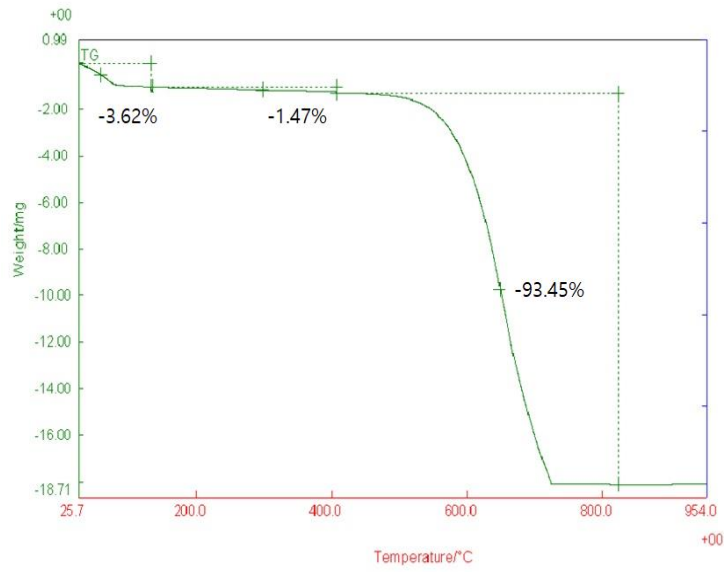


Fig. 1. Thermogravimetric analysis on GAC.

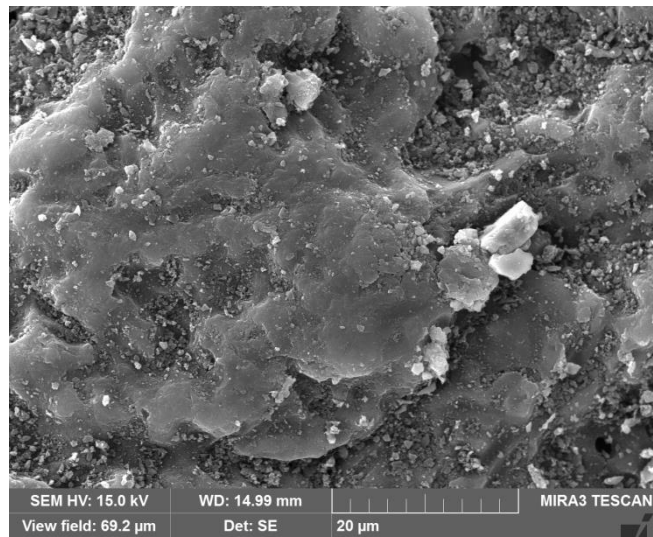


Fig. 2. SEM micrgraph of GAC particles.

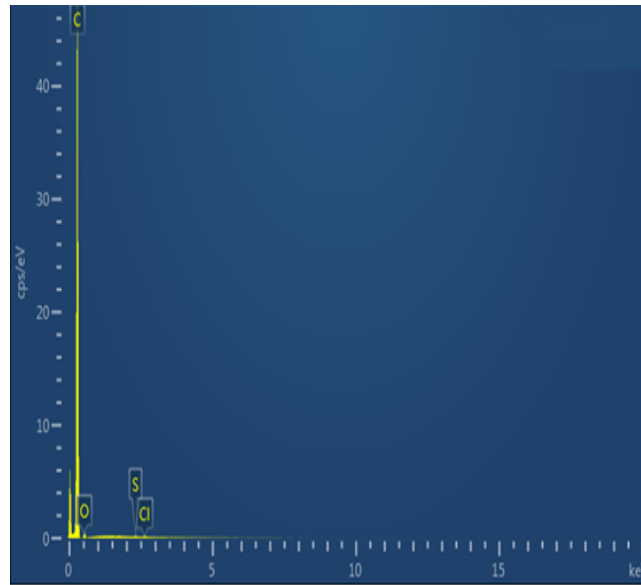


Fig. 3. EDX spectrum of GAC.

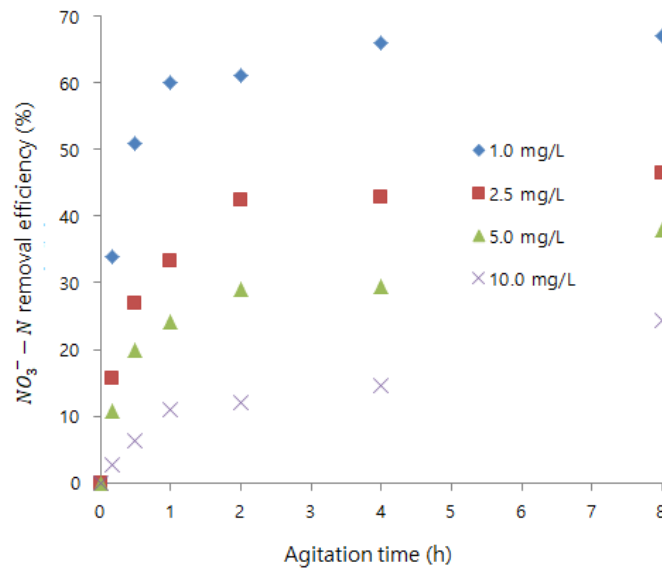


Fig. 4. Removal efficiencies of NO<sub>3</sub><sup>-</sup>-N by GAC at 298 K.

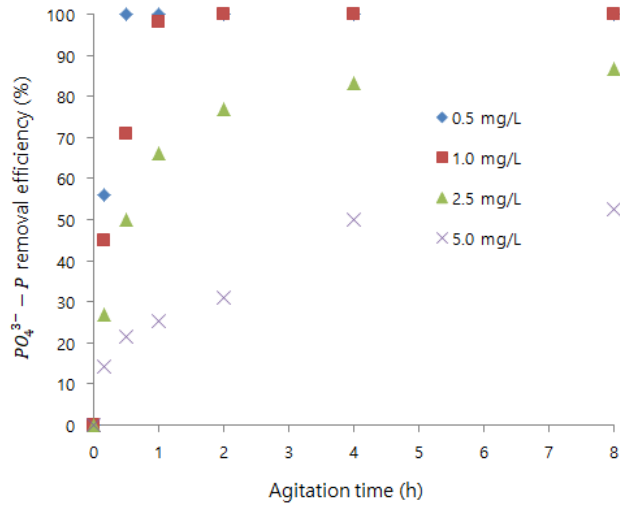


Fig. 5. Removal efficiencies of PO<sub>4</sub><sup>3-</sup>-P by GAC at 298 K.

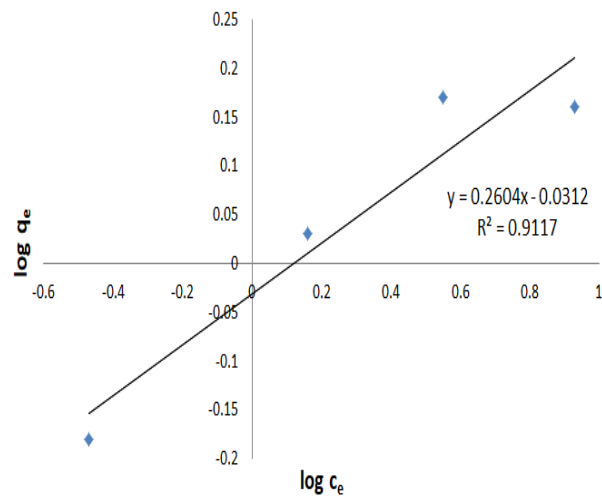


Fig. 6. Freundlich isotherm plot for the adsorption of NO<sub>3</sub><sup>-</sup>-N on GAC.



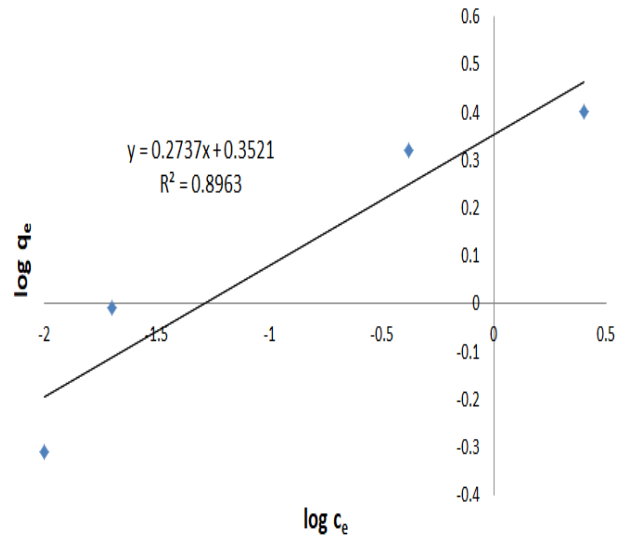


Fig. 7. Freundlich isotherm plot for the adsorption of  $\text{PO}_4^{3-}\text{-P}$  on GAC.

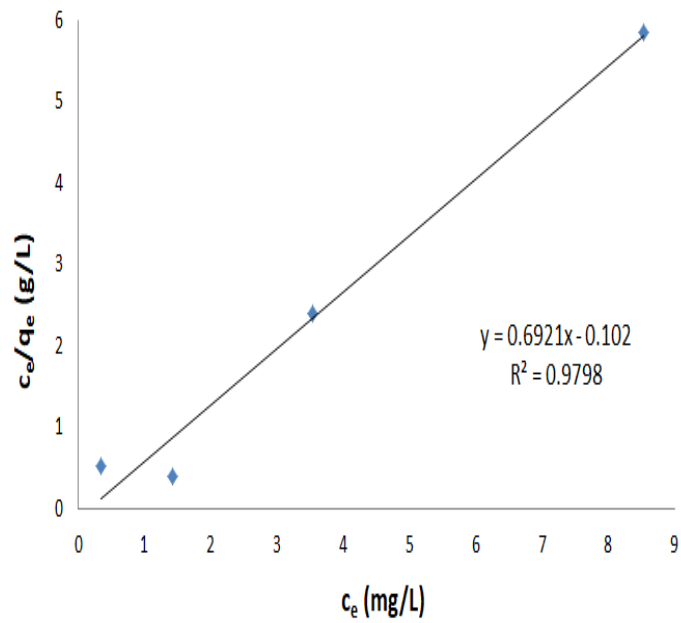


Fig. 8. Langmuir isotherm plot for the adsorption of  $\text{NO}_3^-\text{-N}$  on GAC.

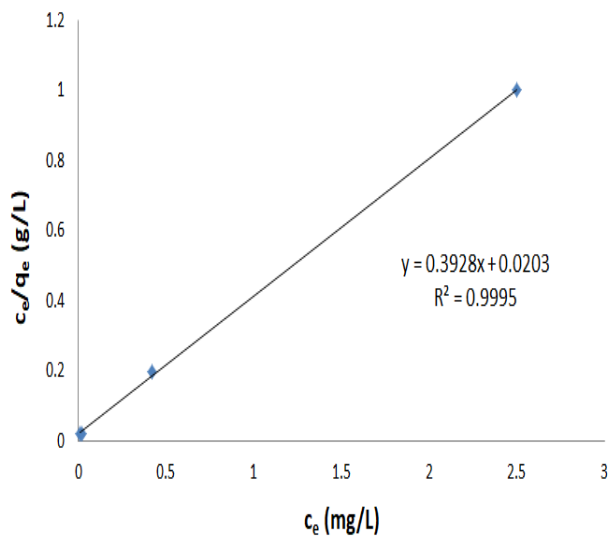


Fig. 9. Langmuir isotherm plot for the adsorption of  $PO_4^{3-}$ -P on GAC.